Design and in Vitro Characterization of Highly sst_2-Selective Somatostatin Antagonists Suitable for Radiotargeting

Renzo Cescato,[†,#] Judith Erchegyi,[‡,#] Beatrice Waser,[†] Véronique Piccand,[†] Helmut R. Maecke,[§] Jean E. Rivier,*[,‡] and Jean Claude Reubi[†]

Division of Cell Biology and Experimental Cancer Research, Institute of Pathology, University of Berne, Berne, Switzerland, The Clayton Foundation Laboratories for Peptide Biology, The Salk Institute for Biological Studies, 10010 N. Torrey Pines Road, La Jolla, California 92037, and Division of Radiological Chemistry, University Hospital Basel, Petersgraben 4, CH-4031 Basel, Switzerland

Received December 21, 2007

Radiolabeled sst_2 and sst_3 antagonists are better candidates for tumor targeting than agonists with comparable binding characteristics (Ginj, M.; Zhang, H.; Waser, B.; Cescato, R.; Wild, D.; Erchegyi, J.; Rivier, J.; Mäcke, H. R.; Reubi, J. C. *Proc. Natl. Acad. Sci. U.S.A.* **2006**, *103*, 16436−16441.). Because most of the neuroendocrine tumors express sst_2, we used the known antagonists acetyl-*p*NO_2Phe^2-*c*[DCys^3-Tyr^7-DTrp^8-Lys^9-Thr^{10}-Cys^{14}]-DTyr^{15}-NH_2 (**1**) (Bass, R. T.; Buckwalter, B. L.; Patel, B. P.; Pausch, M. H.; Price, L. A.; Strnad, J.; Hadcock, J. R. *Mol. Pharmacol*. **1996**, *50*, 709-715. Bass, R. T.; Buckwalter, B. L.; Patel, B. P.; Pausch, M. H.; Price, L. A.; Strnad, J.; Hadcock, J. R. *Mol. Pharmacol*. **1997**, *51*, 170; Erratum.) and H-Cpa^2-*c*[DCys^3-Tyr^7-DTrp^8-Lys^9-Thr^{10}-Cys^{14}]-2Nal^{15}-NH_2 (**7**) (Hocart, S. J.; Jain, R.; Murphy, W. A.; Taylor, J. E.; Coy, D. H. *J. Med. Chem*. **1999**, *42*, 1863−1871.) as leads for analogues with increased sst_2 binding affinity and selectivity. Among the 32 analogues reported here, DOTA-*p*NO_2Phe^2-*c*[DCys^3-Tyr^7-DAph^8(Cbm)-Lys^9-Thr^{10}-Cys^{14}-DTyr^{15}-NH_2 (**3**) and DOTA-Cpa^2-*c*[DCys^3-Aph^7(Hor)-DAph^8(Cbm)-Lys^9-Thr^{10}-Cys^{14}]-DTyr^{15}-NH_2 (**31**) had the highest sst_2 binding affinity and selectivity. All of the analogues tested kept their sst_2 antagonistic properties (i.e., did not affect calcium release in vitro and competitively antagonized the agonistic effect of [Tyr^3]octreotide). Moreover, in an immunofluorescence-based internalization assay, the new analogues prevented sst_2 internalization induced by the sst_2 agonist [Tyr^3]octreotide without being active by themselves. In conclusion, several analogues (in particular **3**, **31**, and **32**) have outstanding sst_2 binding and functional antagonistic properties and, because of their DOTA moiety, are excellent candidates for in vivo targeting of sst_2-expressing cancers.

Introduction

The limitations of therapeutic applications of somatostatin (SRIF[a]) due to its rapid proteolytic degradation and multiple targets have led to the search for peptide analogues with higher metabolic stability and improved selectivity with respect to the five SRIF receptor subtypes. Long-acting preparations of octreotide[5] and lanreotide[6] are now available for use in the treatment of acromegaly, neuroendocrine tumors, and various gastrointestinal disorders. Moreover, targeting neuroendocrine tumors expressing SRIF receptor subtypes with radiolabeled SRIF agonists is an established diagnostic and therapeutic approach in oncology. Somatostatin receptor scintigraphy with ^{111}In-DTPA-octreotide (^{111}In-diethylenetriaminepentaacetyl-octreotide) is the current imaging technique for the localization of neuroendocrine tumors,[7] whereas ^{177}Lu or ^{90}Y-1,4,7,10-tetraazacyclododecane-1,4,7,10-tetraacetyl[Tyr^3]octreotate (^{90}Y-DOTA-TATE) is the radioligand used for tumor radiotherapy.[8,9] Radio-guided surgery for the in situ detection of neuroendocrine tumors during surgery also utilizes ^{111}In-DTPA-octreotide as a tool for tumor localization. The development of more selective analogues with high affinity and enhanced uptake by the SRIF receptor containing tumor cells is expected to open new and more sensitive avenues for radiotherapy and radioguided surgery.[10–12] Classically, this can be achieved using established approaches used for drug design whereby the physicochemical properties of the analogues are systematically modulated leading to stepwise improvements. For example, hydrophobicity, ionic charges, stabilization of secondary structures, and in the case of somatostatin analogues for radiotherapy, exhaustive modifications of the chelator moiety and of the radioactive metal have been reported.[13–19]

While SRIF agonists readily internalize into tumor cells, permitting accumulation of radioactivity, radiolabeled antagonists do not and therefore have not been considered for tumor targeting until recently.[1] We reported that the macrocyclic chelator DOTA-coupled sst_3 and sst_2-selective antagonists did

* To whom correspondence should be addressed. Phone: (858) 453-4100. Fax: (858) 552-1546. E-mail: jrivier@salk.edu.
† University of Berne.
# These authors contributed equally.
‡ The Salk Institute for Biological Studies.
§ University Hospital Basel.

[a] Abbreviations: Agl, aminoglycine; Aph, 4-aminophenylalanine; 3-Br-Bzl, 3-bromobenzyl; Boc, *tert*-butoxycarbonyl; BSA, bovine serum albumin; Bzl, benzyl; Cbm, carbamoyl; Cha, cyclohexylalanine; Cpa, 4-Cl-phenylalanine; CZE, capillary zone electrophoresis; DIC, *N*,*N*′-diisopropylcarbodiimide; DIPEA, *N*,*N*′-diisopropylethylamine; DMEM-LH, Dulbecco's modified Eagle's medium lactalbumine hydrolysate/HEPES; DMF, dimethylformamide; Dod, 4,4′-dimethoxydityl; DOTA, 1,4,7,10-tetraazacyclododecane-1,4,7,10-tetraacetic acid; DTPA, diethylenetriaminepentaacetic acid; ELISA, enzyme-linked immunosorbent assay; Fmoc, 9-fluorenylmethoxycarbonyl; HBSS, Hank's balanced salt solution; HEPES, 4-(2-hydroxyethyl)-1-piperazineethansulfonic acid; HOBt, 1-hydroxybenzotriazole; Hor, L-hydroorotyl; MBHA, methylbenzhydryl resin; Mob, 4-methoxybenzyl; 2Nal, 3-(2-naphthyl)alanine; NMP, *N*-methylpirrolidinone; 3D, three-dimensional; Peg, 12-amino-4,7,10-trioxadodecanoic acid; PBS, phosphate buffered saline; *p*NO_2Phe, *p*-nitrophenylalanine; SAR, structure−activity relationships; SRIF, somatostatin-14; sst_s, SRIF receptors; SRIF-28, somatostatin-28; TATE, [Tyr^3,Thr^8]octreotide = [Tyr^3]octreotate; TEA, triethylamine; TEAP, triethylammonium phosphate; TFA, trifluoroacetic acid; TOC, [Tyr^3]octreotide; Z(2Br), 2-bromobenzyloxycarbonyl; Z(2Cl), 2-chlorobenzyloxycarbonyl. The abbreviations for the common amino acids are in accordance with the recommendations of the IUPAC-IUB Joint Commission on Biochemical Nomenclature (*Eur. J. Biochem*. **1984**, *138*, 9−37). The symbols represent the L-isomer except when indicated otherwise.

10.1021/jm701618q CCC: $40.75
Published on Web 06/11/2008

Table 1. Physicochemical Properties of sst_2 Antagonists

	Structure of SRIF analogues. Residues are numbered according to SRIF numbering H-Ala[1]-Gly[2]-*c*[Cys[3]-Lys[4]-Asn[5]-Phe[6]-Phe[7]-Trp[8]-Lys[9]-Thr[10]-Phe[11]-Thr[12]-Ser[13]-Cys[14]]-OH (SRIF). Substitution in H-DPhe[2]-*c*[Cys[3]-Phe[7]-DTrp[8]-Lys[9]-Thr[10]-Cys[14]]-Thr[15]-ol (octreotide)										purity		MS[c]	
	N-terminus	2	3	7	8	9	10	14	15	C-terminus	HPLC[a]	CZE[b]	M_{calc}	$M + H_{obs}$
1[2]	Ac-	*p*NO_2Phe-	DCys-	Tyr-	DTrp-	Lys-	Thr-	Cys-	DTyr-	NH_2	99	99	1196.44	1197.59
2	DOTA-	*p*NO_2Phe-	DCys-	Tyr-	DTrp-	Lys-	Thr-	Cys-	DTyr-	NH_2	95	97	1540.61	1541.46
3	DOTA-	*p*NO_2Phe-	DCys-	Tyr-	DAph(Cbm)-	Lys-	Thr-	Cys-	DTyr-	NH_2	99	99	1559.63	1560.83
4	H_2N-	*p*NO_2Phe-	DCys-	Tyr-	DAph(Cbm)-	Lys-	Thr-	Cys-	2Nal-	NH_2	99	99	1207.47	1208.54
5	DOTA-	*p*NO_2Phe-	DCys-	Tyr-	DAph(Cbm)-	Lys-	Thr-	Cys-	2Nal-	NH_2	99	99	1593.65	1594.17
6	H_2N-	*p*NO_2Phe-	DCys-	Aph(Hor)-	DAph(Cbm)-	Lys-	Thr-	Cys-	2Nal-	NH_2	99	99	1346.50	1347.59
7[4]	H_2N-	Cpa-	DCys-	Tyr-	DTrp-	Lys-	Thr-	Cys-	2Nal-	NH_2	99	99	1177.43	1178.43
8[27]	H_2N-	Cpa-	DCys-	Tyr-	DTrp-	NMeLys-	Thr-	Cys-	2Nal-	NH_2	97	99	1191.45	1192.52
9	H_2N-	Cpa-	DCys-	L-Agl(NMe,benzoyl)	DTrp-	Lys-	Thr-	Cys-	2Nal-	NH_2	95	98	1204.45	1205.51
10	H_2N-	Cpa-	DCys-	D-Agl(NMe,benzoyl)	DTrp-	Lys-	Thr-	Cys-	2Nal-	NH_2	98	99	1204.45	1205.48
11	H_2N -	Cpa-	DCys-	Leu-	DTrp-	Lys-	Thr-	Cys-	2Nal-	NH_2	99	99	1127.45	1128.46
12	H_2N-	Cpa-	DCys-	Aph(Cbm)-	DTrp-	Lys-	Thr-	Cys-	2Nal-	NH_2	99	97	1219.45	1220.12
13	Cbm-	Cpa-	DCys-	Aph(Cbm)-	DTrp-	Lys-	Thr-	Cys-	2Nal-	NH_2	96	98	1262.46	1263.40
14	DOTA-	Cpa-	DCys-	Aph(Cbm)-	DTrp-	Lys-	Thr-	Cys-	2Nal-	NH_2	99	98	1605.64	1606.50
15	DOTA-βAla-	Cpa-	DCys-	Aph(Cbm)-	DTrp-	Lys-	Thr-	Cys-	2Nal-	NH_2	99	98	1676.67	1677.67
16	DOTA-Peg-	Cpa-	DCys-	Aph(Cbm)-	DTrp-	Lys-	Thr-	Cys-	2Nal-	NH_2	99	99	1809.62	1810.24
17	H_2N-	Cpa-	DCys-	Aph(Cbm)-	DTrp-	Lys-	Thr-	Cys-		NH_2	99	99	1022.37	1023.49
18	H_2N-	Cpa-	DCys-	Aph(Cbm)-	DTrp-	Lys-	Thr-	Cys-	Cha-	NH_2	99	96	1175.48	1176.36
19	H_2N-	Cpa-	DCys-	Aph(Cbm)-	DTrp-	Lys-	Thr-	Cys-	Aph(Hor)-	NH_2	99	99	1324.47	1325.55
20	H_2N-	Cpa-	DCys-	Aph(Cbm)-	DTrp-	Lys-	Thr-	Cys-	DAph(Cbm)-	NH_2	99	99	1227.45	1228.45
21	H_2N-	Cpa-	DCys-	Aph(Cbm)-	DTrp-	Lys-	Thr-	Cys-	Aph(Cbm)-	NH_2	99	99	1227.45	1228.37
22	H_2N-	Cpa-	DCys-	Aph(Cbm)-	DTrp-	Lys-	Thr-	Cys-	DAph(Cbm)-	Gly-OH	98	98	1285.46	1286.34
23	H_2N-	Cpa-	DCys-	Aph(CONH-OCH_3)-	DTrp-	Lys-	Thr-	Cys-	2Nal-	NH_2	99	99	1249.46	1250.56
24	H_2N-	Cpa-	DCys-	Aph(CONH-OH)-	DTrp-	Lys-	Thr-	Cys-	2Nal-	NH_2	99	99	1235.44	1236.47
25	H_2N-	Cpa-	DCys-	Aph(Cbm)-	5F-DTrp-	Lys-	Thr-	Cys-	2Nal-	NH_2	96	96	1237.44	1238.44
26	H_2N-	Cpa-	DCys-	Aph(Cbm)-	5F-Trp-	Lys-	Thr-	Cys-	2Nal-	NH_2	96	85	1237.44	1238.24
27	H_2N-	Cpa-	DCys-	Tyr-	DAph(Cbm)-	Lys-	Thr-	Cys-	2Nal-	NH_2	99	99	1196.43	1197.36
28	DOTA-	Cpa-	DCys-	Tyr-	DAph(Cbm)-	Lys-	Thr-	Cys-	2Nal-	NH_2	99	99	1582.62	1583.72
29	H_2N-	Cpa-	DCys-	Aph(Hor)-	DAph(Cbm)-	Lys-	Thr-	Cys-	2Nal-	NH_2	91	95	1335.47	1336.44
30	DOTA-	Cpa-	DCys-	Aph(Hor)-	DAph(Cbm)-	Lys-	Thr-	Cys-	2Nal-	NH_2	95	94	1721.65	1722.56
31	DOTA-	Cpa-	DCys-	Aph(Hor)	DAph(Cbm)-	Lys-	Thr-	Cys-	DTyr-	NH_2	96	97	1687.64	1688.83
32	DOTA-	*p*NO_2Phe-	DCys-	ITyr-	DTrp-	Lys-	Thr-	Cys-	DTyr-	NH_2	99	99	1666.52	1667.74

[a] Percent purity determined by HPLC using buffer system: A = TEAP (pH 2.5) and B = 60% CH_3CN/40% A with a gradient slope of 1% B/min, at flow rate of 0.2 mL/min on a Vydac C_{18} column (0.21 cm × 15 cm, 5 μm particle size, 300 Å pore size). Detection at 214 nm. [b] Capillary zone electrophoresis (CZE) was done using a Beckman P/ACE system 2050 controlled by an IBM Personal System/2 model 50Z and using a ChromJet integrator. Field strength of 15 kV at 30 °C. Mobile phase: 100 mM sodium phosphate (85:15, H_2O/CH_3CN), pH 2.50, on a Supelco P175 capillary (363 μm OD μm × 75 μm i.d. × 50 cm length). Detection at 214 nm. [c] The calculated *m/z* of the monoisotope compared with the observed $[M + H]^+$ monoisotopic mass.

not trigger sst_3 or sst_2 internalization, prevented agonist-stimulated internalization; yet they were excellent in vivo tumor markers.[1,20] Potent agonists with strong binding and internalization properties showed a much lower and shorter-lasting uptake in SRIF receptor-expressing tumors than the tested antagonists. The amount of uptake of the antagonist radioligand was particularly high in the tested tumors: 60% IA/g uptake has indeed never been achieved before by any radiolabeled SRIF receptor agonist, not even by those developed most recently.[11,12] Not only was the uptake at the peak time point very high but also the long-lasting accumulation of the antagonist radioligand up to 72 h after injection was a remarkable result and represented a considerable advantage over radiotargeting with established agonists. We concluded that SRIF antagonist radiotracers are therefore preferable over agonists for the in vivo targeting of sst_3- or sst_2-expressing tumors. The use of potent radiolabeled antagonists for in vivo tumor targeting may considerably improve the sensitivity of diagnostic procedures, the staging of the disease, the detection of unexpected tumor sites, and the efficacy of receptor-mediated radiotherapy and complementary procedures.[10,21–23]

To generate pure sst_2 antagonists for therapeutic applications and because the great majority of neuroendocrine tumors express predominantly sst_2, we have focused the present study on the development of potent, highly sst_2-selective unlabeled and DOTA-labeled antagonists. This was achieved with the introduction of novel amino acid derivatives within the sequence of octreotide amide and documented with binding assays to the five human sst_s and several functional assays such as internalization assays and calcium release.

Results and Discussion

All of the analogues shown in Table 1 were synthesized either manually or automatically on a MBHA resin using the Boc strategy, diisopropylcarbodiimide (DIC)/HOBt (1-hydroxybenzotriazole) for amide bond formation and trifluoroacetic acid (TFA) for Boc removal. The peptide resins were treated with hydrogen fluoride (HF) in the presence of scavengers to liberate the fully deprotected crude linear peptides. Cyclization of the cysteines was mediated by iodine in an acidic milieu. Purification was carried out using multiple HPLC steps.[24] DOTA was coupled to the Lys(Fmoc)[9] protected analogues in solution. The purity of the peptides was characterized by HPLC,[24] capillary zone electrophoresis,[25] and mass spectrometry. The observed monoisotopic mass $(M + H)^+$ values of each peptide correspond to the calculated mass (M) values. Results are shown in Table 1.

To investigate their sst_s-binding properties, the peptides were tested for their ability to bind to cryostat sections from membrane pellets of cells expressing the five human sst_s (Table 2). For each of the tested compounds, complete displacement experiments were carried out with the universal SRIF radioligand [Leu[8],DTrp[22], ^{125}I-Tyr[25]]SRIF-28. Results are shown in Table 2.

Inverting chirality at positions 2 and 3 in the octreotide scaffold (H-DPhe[2]-*c*[Cys[3]-Phe[7]-DTrp[8]-Lys[9]-Thr[10]-Cys[14]]-Thr[15]-

Table 2. sst_{1-5} Binding Affinities (IC_{50}, nM) and Function of sst_2-Selective Analogues

	IC_{50} (nM)[a]					functional characterization	
	sst_1	sst_2	sst_3	sst_4	sst_5	sst_2 internalization	calcium assay
SRIF-28	2.7 ± 0.2	2.7 ± 0.2	3.3 ± 0.4	2.6 ± 0.4	2.4 ± 0.2		
1	>1000	3.6 ± 0.4	>1000	349 ± 30	276 ± 119	antagonist	
2	>1000	1.5 ± 0.4	>1000	287 ± 27	>1000	antagonist	antagonist
3	>1000	0.75 ± 0.2	>1000	>1000	>1000	antagonist	antagonist
4	>1000	2.6 ± 0.7	384 ± 97	>1000	>1000	antagonist	
5	>1000	1.3 ± 0.2	>1000	>1000	>1000	antagonist	antagonist
6	>1000	2.7 ± 0.6	451 ± 80	>1000	>1000		
7	>1000	5.7 ± 1.5	112 ± 32	296 ± 19	218 ± 63	antagonist	antagonist
8	>1000	10 ± 3.5	61 ± 14	715 ± 137	53 ± 19	antagonist	antagonist
9	>1000	17 ± 5	827 ± 244	>1000	442 ± 254	antagonist	
10	>1000	158 ± 37	102 ± 10	116 ± 47	728 ± 272		
11	>1000	58 ± 21	340 ± 77	908 ± 138	657 ± 299		
12	>1000	6.9 ± 0.7	155 ± 29	479 ± 8	149 ± 37	antagonist	antagonist
13	>1000	23 ± 4.3	54 ± 15	136 ± 7.5	111 ± 17		
14	>1000	9.8 ± 1.2	972 ± 212	831 ± 82	>1000	antagonist	antagonist
15	>1000	46 ± 13	124 ± 53	>1000	>1000	antagonist	antagonist
16	>1000	40 ± 1.5	88 ± 13	728 ± 158	895 ± 294	antagonist	
17	>1000	5.9 ± 1.8	138 ± 52	>1000	461 ± 106	antagonist	antagonist
18	>1000	4.1 ± 0.9	255 ± 79	>1000	247 ± 66		
19	>1000	27 ± 3.8	162 ± 19	>1000	320 ± 69		
20	>1000	5.4 ± 1	328 ± 69	800 ± 295	191 ± 49		
21	>1000	15 ± 3	336 ± 46	551 ± 151	560 ± 144		
22	>1000	52 ± 4.7	661 ± 115	>1000	810 ± 200		
23	>1000	9.3 ± 0.9	157 ± 49	883 ± 174	313 ± 35		
24	>1000	9.3 ± 1.4	120 ± 45	813 ± 152	426 ± 189		
25	>1000	4.9 ± 1.5	50 ± 5.8	287 ± 64	94 ± 34	antagonist	antagonist
26	>1000	23 ± 3.7	90 ± 11	905 ± 132	618 ± 248		
27	>1000	3.7 ± 1.3	346 ± 81	>1000	>1000		
28	>1000	1.4 ± 0.5	>1000	>1000	>1000	antagonist	antagonist
29	>1000	2.4 ± 0.6	83 ± 2.0	>1000	>1000	antagonist	antagonist
30	>1000	1.7 ± 0.2	>1000	>1000	>1000	antagonist	antagonist
31	>1000	0.7 ± 0.12	>1000	>1000	>1000	antagonist	antagonist
32	>1000	1.2 ± 0.4	>1000	455 ± 125	>1000	antagonist	antagonist

[a] The IC_{50} values (nM) were derived from competitive radioligand displacement assays reflecting the affinities of the analogues for the cloned SRIF receptors using the nonselective [Leu^8,DTrp^{22},^{125}I-Tyr^{25}]SRIF-28, as the radioligand. Mean value ± SEM for $n \geq 3$.

ol, SRIF numbering) was reported to be the key structural modification converting an SRIF agonist into an antagonist.[2,3] Additional substitutions resulted in partially selective antagonists acetyl-*p*NO_2Phe-*c*[DCys-Tyr-DTrp-Lys-Thr-Cys]-DTyr-NH_2[2] or H-Cpa-*c*[DCys-Tyr-DTrp-Lys-Thr-Cys]-2Nal-NH_2.[4] These antagonists display preferentially high binding affinity for sst_2 and lower or no affinity to sst_3, sst_4, and sst_5. None of the analogues bind to sst_1. Using these lead compounds, we have designed SRIF antagonists that were more affine (>3-fold) and more sst_2-selective than those reported so far. Guided by earlier observations whereby amide bond-rich moieties are favorably recognized by GPCR, most of the analogues reported have carbamoyl functionalities.[26] We believe that this empirically based approach to drug design is to be distinguished from what is referred to as SAR studies. Indeed, a state-of-the-art and comprehensive SAR study will include conformational considerations, whereas a "drug design" strategy may be based on intuitive, systematic, and iterative substitutions, an understanding (although partial) of the fundamentals of peptide/protein interactions, deletions and changes in chirality among others, with the exclusion of structural requirements. On the other hand, it is only with the knowledge of the 3D NMR structures of the improved, structurally constrained, and bioactive analogues resulting from such empirical strategies (applying a drug design approach) that a consensus pharmacophore can be determined (Grace et al., submitted) and used for true SAR. This is exemplified in a manuscript to be submitted elsewhere (Erchegyi et al., in preparation).

This being said, analogues of antagonists like acetyl-*p*NO_2Phe^2-*c*[DCys^3-Tyr^7-DTrp^8-Lys^9-Thr^{10}-Cys^{14}]-DTyr^{15}-NH_2[2] (**1**) and H-Cpa^2-*c*[DCys^3-Tyr^7-DTrp^8-Lys^9-Thr^{10}-Cys^{14}]-2Nal^{15}-NH_2[4] (**7**) were synthesized to investigate the effect of different substitutions on binding affinity, receptor-subtype selectivity, overall hydrophilicity, agonism, and antagonism.

The substitution of the N-terminal acetyl group by DOTA in **1** (IC_{50} = 3.6 nM at sst_2) resulted in **2**, which bound to sst_2 with IC_{50} = 1.5 nM, suggesting that the DOTA moiety, which is crucial for radiolabeling with ^{111}In, ^{90}Y, or ^{177}Lu for in vivo targeting, is well tolerated by sst_2 (Table 2). This conclusion is confirmed further with several additional examples. The introduction of DAph(Cbm)^8 in place of DTrp^8 in **2** yielded **3** (IC_{50} = 0.75 nM). It is noteworthy that these two substitutions are cumulative, thus resulting in the most potent sst_2 antagonist in this series, with no measurable binding affinity to any of the other receptors. Further replacement of DTyr^{15} in **3** by 2Nal^{15} yielded **5** with a similar binding affinity for sst_2 (IC_{50} = 1.3 nM). Analogue **4**, a peptide with the same sequence as **5** but without DOTA at its N-terminus, still had excellent binding affinity for sst_2 (IC_{50} = 2.6 nM) and also bound measurably to sst_3 (IC_{50} = 384 nM). Substitution of Tyr in position 7 by Aph(Hor) resulting in **6** had no effect on sst_2 binding affinity and selectivity when compared with the parent **4** (IC_{50} of 2.6 and 2.7 nM at sst_2 and IC_{50} of 384 and 451 nM at sst_3, respectively, and no binding affinity at the other three receptors) (Table 2).

We also used H-Cpa^2-*c*[DCys^3-Tyr^7-DTrp^8-Lys^9-Thr^{10}-Cys^{14}]-2Nal^{15}-NH_2 (**7**) published by Hocart et al.[4] as a second lead for sst_2-selective antagonists. This antagonist has IC_{50} values in our binding assay equal to 5.7, 112, and 218 nM at $sst_{2/3/5}$, respectively, compared to the reported K_i values of 26, 93, and 48 nM. In our assays, **7** is more potent than reported at sst_2 by a factor of 5 and less potent at sst_5 by the same factor. This

points to the danger of comparing results from one laboratory to another when engaged in SAR studies.

Whereas N^{α}-methylation of Lys^9 in **7**[4] to yield **8**[27] increased sst_2 binding affinity by a modest 5-fold in the assay used by Hocart et al.[4] (K_i = 26 and 5.51 nM, respectively) with no improvement at sst_3 or sst_5 ($K_i \approx 50-100$ nM), our in vitro binding assay could not confirm this improvement at sst_2, and as a result, we did not pursue the use of this substitution in the design of additional sst_2-selective analogues. Instead, we synthesized **9** with an L-Agl(NMe,benzoyl)[7] in an attempt to constrain the orientation of the side chain at position 7. The use of such aminoglycine derivatives (betides)[28,29] had been taken advantage of in the design of an sst_3-selective antagonist.[30,31] While **9** lost some binding affinity for sst_2 (3-fold) compared to **7**, it also lost comparable binding affinity for sst_3 and sst_5. This observation further suggests that position 7 is critical for all three $sst_{2,3,5}$. In fact, **10** with the D-Agl(NMe,benzoyl)[7] lost binding affinity at sst_2 while retaining similar binding affinities as **7** at $sst_{3/4/5}$, thus accomplishing one of our goals of identifying those residues/conformations responsible for binding to any particular receptor (i.e., sst_2 in this case).

Whereas substitution of Tyr by Leu at position 7 in **7** yielded **11**, which lost 10-fold binding affinity for sst_2 and selectivity, substitution by Aph(Cbm) yielded **12** which exhibited similar binding affinity and selectivity as **7** at the five sst_s. N-terminal carbamoylation of **12** to yield **13** improved binding affinity slightly at $sst_{3/4}$ with some loss of binding affinity for sst_2 compared to **12**. Addition of DOTA to **12** resulted in **14** whose sst_2 binding affinity is similar to that of **12** and increased selectivity for sst_2.

Interestingly, addition of a spacer in **14** between DOTA and the octapeptide such as βAla in **15** and Peg in **16** was unexpectedly detrimental[32,33] in terms of sst_2 binding affinity, yet favorable for sst_3 and neutral at $sst_{1/4/5}$.

From our observation that $2Nal^{15}$ may contribute to the sst_3, sst_4, and sst_5 binding pocket, **17** (missing this residue) was synthesized and found to have similar binding affinities when compared to the parent **12**. Substitution of $2Nal^{15}$ in **12** by other different residues such as Cha in **18**, Aph(Hor) in **19**, DAph(Cbm) in **20**, and Aph(Cbm) in **21** did not markedly influence affinity at sst_2 or selectivity. This is noteworthy in that there is only a 3-fold difference in binding affinity at sst_2 for **20** (D-configuration and IC_{50} = 5.4 nM) and **21** (L-configuration and IC_{50} = 15 nM) where the C-terminal amino acid is of the D or L configuration. This supports the earlier observation that DTyr (as in **1** and **2**) or 2Nal (as in **4** and **5**) are both equally accepted. On the other hand, extension of the sequence of **20** by Gly-OH as in **22** leads to significant loss of affinity at all receptors.

In order to modulate the overall hydrophilicity of **7** (with Tyr at position 7), we introduced the following carbamates ($Aph(Cbm)^7$) in **12**, ($Aph(CONH\text{-}OCH_3)^7$) in **23**, and ($Aph(CONH\text{-}OH)^7$) in **24** at position 7. Whereas binding affinities for these analogues are not different from that of the parent **7**, the order of elution of these analogues on HPLC at neutral pH suggests that **24** (t_R = 31.6 min) may be more hydrophilic than **7** (t_R = 34.8 min), **12** (t_R = 31.9 min), and **23** (t_R = 34.2 min). Since hydrophilicity may be a critical criterion for a clinically relevant radioligand, subtle differences in structure may favor one of these analogues when selecting a clinical candidate. The fact that **12**, **23**, and **24** are not superior to **7** in terms of sst_2 binding affinity and selectivity supports our previous finding that residue 7 is not an essential contributor to the sst_2 pharmacophore.[34]

We then investigated the effect of substitutions at position 8. There is literature precedent suggesting that 5F-Trp is a favorable substitution for Trp^8.[35] When introduced in **12** to yield **25** and **26**, we observed a slight improvement in binding affinity for the three $sst_{2/3/5}$ as expected for the 5F-DTrp-containing **25** and less so for the corresponding L-isomer-containing **26**. No increase in selectivity, however, was seen for either analogue.

It was therefore very rewarding to find out that substitution of $DTrp^8$ in **7** by $DAph(Cbm)^8$ yielding **27** was clearly superior in terms of sst_2 selectivity with improved binding affinity. Further derivatization with the addition of DOTA at the N-terminus yielded **28** with an additional increase in binding affinity to sst_2 and greater than 500-fold selectivity at all other receptors.

Substitution of Tyr^7 in **27** and **28** with Aph(Hor) yielded **29** and **30**. Whereas **29** retained high binding affinity at sst_2, it also exhibited moderate binding affinity for sst_3; the binding affinity at sst_3 was lost upon the introduction of DOTA (**30**). Substitution of Tyr^7 in **2** with ITyr yielded **32**, the binding affinity of which was similar to that of **2** at sst_2.

We then substituted $2Nal^{15}$ in **30** by $DTyr^{15}$ to yield **31**. Of all analogues presented here, **31** (because of its hydrophilicity, t_R = 13.2 min) may be the preferred candidate for biodistribution and ultimately clinical investigation over **3** (t_R = 13.6 min), **5** (t_R = 26.1 min), **28** (t_R = 26.7 min), **30** (t_R = 26.7 min), or **32** (t_R = 25.0 min) that are equally potent and selective in the binding assay. It is remarkable that the dipeptide sequence -Aph(Hor)-DAph(Cbm)- found in **29**−**31** is identical to that found in degarelix (Fe-200486),[26] a gonadotropin releasing hormone antagonist where it played a critical role in stabilizing a turn and in extending duration of action.

Put in perspective, the most affine DOTA-containing antagonists presented here (**3** and **31**) have binding affinities 3- to 4-fold higher than SRIF-28 with no detectable binding affinity at any of the other four sst_s and are therefore potential candidates for clinical use.

All of the analogues tested here are antagonists in the calcium release assay in HEK293 cells stably expressing the human sst_2. When tested alone, they do not affect calcium release up to 10 μM. However, the agonistic effect of the sst_2 agonist [Tyr^3]octreotide can be competitively antagonized with a 100-fold excess of each of the analogues applied individually. Figure 1 illustrates the antagonistic properties of some of the sst_2 antagonists using the calcium release assay.

The antagonistic property of the analogues **3**, **31**, and **32** was also confirmed in an immunofluorescence-based internalization assay[20] with HEK293 cells stably expressing the human sst_2. Figure 2 illustrates that although the control agonist [Tyr^3]octreotide can induce sst_2 internalization, the tested sst_2-selective antagonists have no effect when given alone, even at a concentration of 10 μM. Moreover, they prevent sst_2 internalization induced by [Tyr^3]octreotide. Figure 3 shows the antagonistic properties of another analogue (**32**) in the ELISA internalization assay.

To conclude, a great majority of the analogues reported here have a high affinity binding in the nanomolar range for sst_2 and often a high selectivity for sst_2 as well. The best compounds were **3** and **31** (with IC_{50} values below 1 nM) followed by **32**, **5**, **28**, **2**, and **30**. All of these antagonists are of particular interest, since they all include a DOTA moiety, making them candidates for in vivo tumor targeting. The labeling properties of the analogues and the specific in vivo uptake in tumors will be

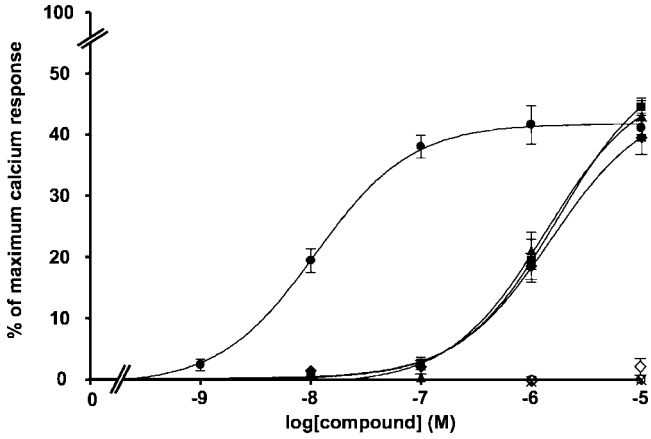

Figure 1. The SRIF analogues **3**, **31**, and **8** behave like antagonists when tested in the calcium release assay. The calcium release assay was performed as described in Experimental Section. HEK-sst$_2$ cells were treated with 1 nmol/L, 10 nmol/L, 100 nmol/L, 1 μmol/L, and 10 μmol/L [Tyr^3]octreotide (●) alone or with 10 nmol/L, 100 nmol/L, 1 μmol/L, and 10 μmol/L [Tyr^3]octreotide in the presence of an increasing concentration (10 nmol/L, 100 nmol/L, 1 μmol/L, and 10 μmol/L) of **3** (■) or **31** (▲) or the specific sst$_2$-antagonist **8** (◆). **3**, **31**, and **8** are antagonists because they shift the dose−response curve of [Tyr^3]octreotide to a higher molar range. Tested alone at 1 and 10 μmol/L **3** (×), **31** (○) and **8** (◇) have no effect on calcium release in HEK-sst$_2$ cells.

discussed in a subsequent publication (Maecke et al., in preparation).

Experimental Section

Starting Materials. MBHA resin with a capacity of 0.3−0.4 mequiv/g was used in the solid phase syntheses. All Boc-N$^\alpha$-protected amino acids with side chain protection, Cys(Mob), Lys(ε-2Cl-Z), Lys(Fmoc), Thr(Bzl), Tyr(2Br-Z), and ITyr(3Br-Bzl) are commercially available (Bachem Inc., Torrance, CA; Chem Impex, Wood Dale, IL; Reanal, Budapest, Hungary) except Boc-Aph-(Cbm)-OH, Boc-DAph(Cbm)-OH, Boc-Aph(Cbm-OCH$_3$)-OH, Boc-Aph(Cbm-OH)-OH, Boc-Aph(Hor)-OH,[26] Fmoc-D/L-Agl(NMe,Boc)-OH,[28] Fmoc-D-Agl(Boc)-OH,[36] Boc-5F-Trp-OH, Boc-5F-DTrp-OH, which were synthesized in our laboratory. 1,4,7,10-Tetraazacyclododecane-1,4,7,10-tetraacetic acid mono(*N*-hydroxysuccinimide)·ester·3CH$_3$COOH·HPF$_6$ (DOTA-NHS) was purchased from Macrocyclics Inc. (Dallas, TX). All reagents and solvents were ACS grade and were used without further purification.

Peptide Synthesis. Peptides were synthesized by the solid-phase approach either manually or on a CS-Bio Peptide Synthesizer Model CS536.[37] A 3 equiv excess of Boc-amino acid (1.2 mmol) based on the original substitution of the resin was used for each coupling. Peptide couplings were mediated for 1 h by DIC/HOBt (1.2 mmol/1.8 mmol) in dimethylformamide (DMF) and monitored by the qualitative ninhydrin test.[38] Boc removal was achieved with trifluoroacetic acid (TFA) (60% in CH_2Cl_2, 1−2% ethanedithiol or *m*-cresol) for 20 min. An isopropyl alcohol (1% *m*-cresol) wash followed TFA treatment, and then successive washes with triethylamine (TEA) solution (10% in CH_2Cl_2), methanol, triethylamine solution, methanol, and CH_2Cl_2 completed the neutralization sequence. The ureido group (Cbm) at the N-terminus of **13** was introduced on the resin. The N-terminal Boc group of the fully assembled peptide was deprotected with TFA in the usual manner.[26] After neutralization, the carbamoylation proceeded with NaOCN (100 mg, 0.65 mmol) in *N*-methylpirrolidinone (NMP) (4 mL) and glacial acetic acid, 3 mL per gram of initial resin. The mixture was agitated at room temperature for 30 min, and the ninhydrin test indicated a complete reaction. The completed peptide was then unprotected and cleaved from the resin by HF containing the scavengers anisole (10% v/v) and methyl sulfide (5% v/v) for 60 min at 0 °C. The diethyl ether precipitated crude peptides were cyclized in 75% acetic acid (200 mL) by addition of iodine (10% solution in methanol) until the appearance of a stable orange color. Forty minutes later, ascorbic acid was added to quench the excess of iodine.

For the synthesis of **9**, we used unresolved Fmoc-D/L-Agl(N-Me,Boc)-OH, and the two diastereomers were separated readily during the standard HPLC purification steps.[24,39] The optical configuration of the two diastereomers was tentatively inferred from a comparison of the HPLC elution behavior with analogue synthesized separately as diastereomers of known optical configuration. In short, after Fmoc-DAgl(Boc)-OH in position 7 was coupled, the side chain protecting Boc group was removed with 60% TFA, washed, and neutralized. To the 0.9 g peptide resin (0.36 mmol/g) swollen in dichloromethane, Dod-Cl (130 mg, 0.5 mmol) was added along with DIEPA (500 μL). The mixture was shaken for an hour to complete the alkylation. The resin was washed and shaken after the addition of formaldehyde (2 mL, 37% solution) in NMP (18 mL) and acetic acid (100 μL). After 5 min, sodium cyanoborohydride (300 mg) was added and the mixture was shaken for 60 min. After the removal of the Dod group with TFA (60%) for 30 min, benzoyl chloride (500 μL) was used to acylate the free secondary amino group of the side chain.[40] Removal of the N$^\alpha$-Fmoc protecting group with 20% piperidine in NMP in two successive 5 and 15 min treatments was followed by the standard elongation protocol until completion of the peptide. The peptide was cleaved, deprotected, and cyclized as described above. On HPLC, this D configuration diastereomer coeluted with the ealier eluting diastereomer from the synthesis performed with the unresolved amino acid; therefore, the slower eluting peptide (**9**) was tentatively identified as the L-Agl(NMe, benzoyl)[7] containing analogue.

Generally, for the synthesis of the DOTA−peptide conjugates, the side chain of Lys^9 was protected with an Fmoc protecting group that stays on after HF cleavage. To a solution of the RP-HPLC purified [Lys(Fmoc)^9]-sst$_2$-antagonist (~20 μM) in dry DMF (800 μL) was added a solution of DOTA-NHS-ester (38 mg, 48 μM) in DMF (160 μL) and *N*,*N*′-diisopropylethylamine (DIPEA) (40 μL, 24 μM). The mixture was stirred at room temperature for 5 h. The progress of the reaction was followed by analytical HPLC. After completion of the reaction, a preparative RP-HPLC purification was performed, yielding the pure DOTA-[Lys(Fmoc)]^9-sst$_2$-antagonist. Removal of the Fmoc protecting group from the Lys side chain was achieved with 20% piperidine/DMF solution resulting in the DOTA-sst$_2$-antagonist, which was further purified by preparative RP-HPLC.

Purification of Peptides. The crude, lyophilized peptides were purified by preparative RP-HPLC[24] on a 5 cm × 30 cm cartridge, packed in the laboratory with reversed-phase 300Å Vydac C$_{18}$ silica (15−20 μm particle size). The peptides eluted with a flow rate of 100 mL/min using a linear gradient of 1% B per 3 min increase from the baseline % B (eluent A = 0.25 N TEAP, pH 2.25; eluent B = 60% CH$_3$CN, 40% A). All peptides were subjected to a second purification step carried out with eluents A = 0.1% TFA in water and B = 60% CH$_3$CN/40% A on the same cartridge using a linear gradient of 1% B per min increase from the baseline % B. Analytical HPLC screening of the purification was performed on a Vydac C$_{18}$ column (0.46 cm × 25 cm, 5 μm particle size, 300 Å pore size) connected to a Rheodyne injector, two Waters pumps model 501, system controller programmer, Kratos 750 UV detector, and Houston Instruments D-5000 strip chart recorder. The fractions containing the product were pooled and subjected to lyophilization.

Characterization of SRIF Analogues (Table 1). The purity of the final peptides was determined by analytical RP-HPLC performed with a linear gradient using 0.1 M TEAP, pH 2.5, as eluent A and 60% CH$_3$CN/40% A as eluent B on a Hewlett-Packard series II 1090 liquid chromatograph connected to a Vydac C$_{18}$ column (0.21 cm × 15 cm, 5 μm particle size, 300 Å pore size), controller model 362, and a Think Jet printer. Capillary zone electrophoresis (CZE) analysis was performed as described earlier.[25] Each peptide was found to have a purity of >95% by HPLC and CZE. Mass spectra (MALDI-MS) were measured on an ABI-Perseptive DE-STR

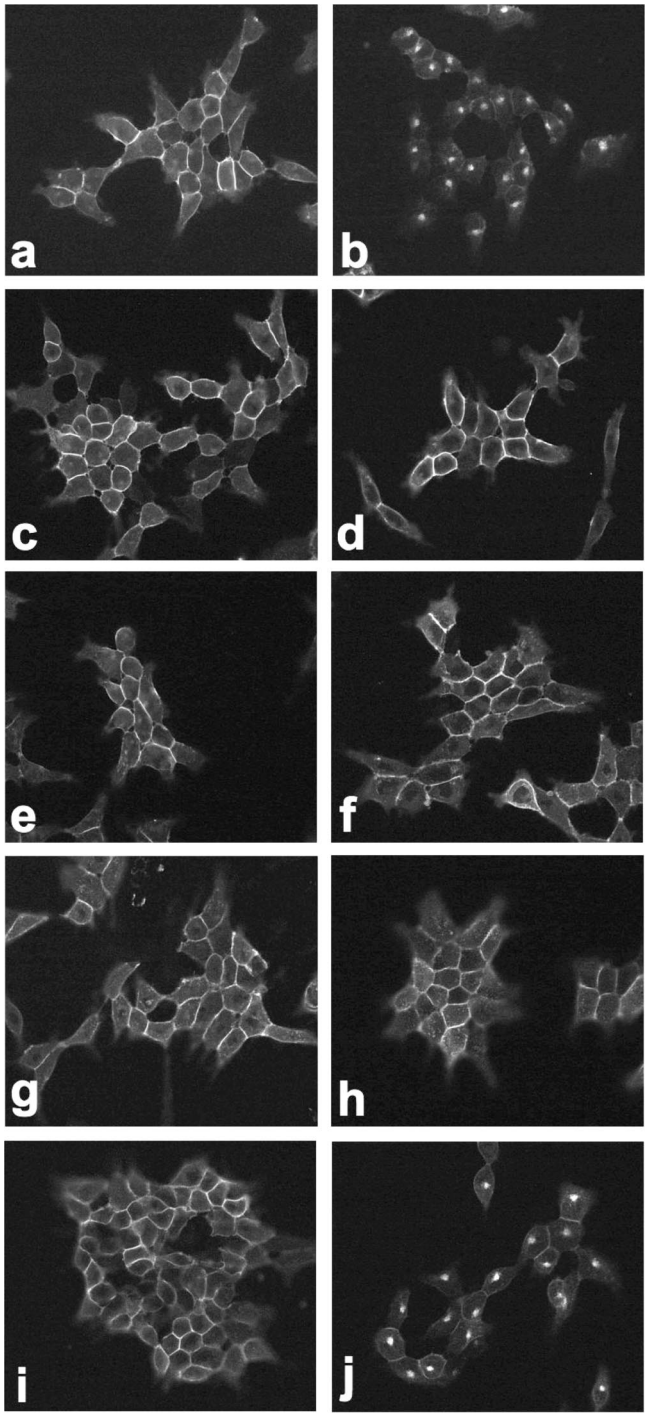

Figure 2. The sst$_2$ internalization induced by [Tyr^3]octreotide is efficiently antagonized by the three SRIF analogues **32**, **3**, and **31**. The immunofluorescence-based internalization assay was performed as described in Experimental Section. HEK-sst$_2$ cells were treated for 30 min either with vehicle (no peptide, panel a) or with 100 nmol/L [Tyr^3]octreotide (panel b), a concentration inducing a submaximal internalization effect. Panels d, f, h show HEK-sst$_2$ cells treated with 100 nmol/L [Tyr^3]octreotide in the presence of 10 μmol/L **32**, **3**, and **31**. The effect of **32**, **3**, and **31** alone at a concentration of 10 μmol/L is shown in panels c, e, g. As controls, panel i shows cells treated with 100 nmol/L [Tyr^3]octreotide in the presence of 10 μmol/L of the specific sst$_2$-antagonist **8**, and panel j shows cells treated with 100 nmol/L [Tyr^3]octreotide in the presence of 10 μmol/L sst$_3$-antagonist sst$_3$-ODN-8. A clear punctate perinuclear staining is detectable for [Tyr^3]octreotide. This punctate staining is efficiently abolished by an excess of the analogues **32**, **3**, **31,** as well as the established antagonist **8**. However, **32**, **3**, and **31** given alone have no effect on sst$_2$ internalization. sst$_3$-ODN-**8**, as negative control, is not able to antagonize the [Tyr^3]octreotide effect.

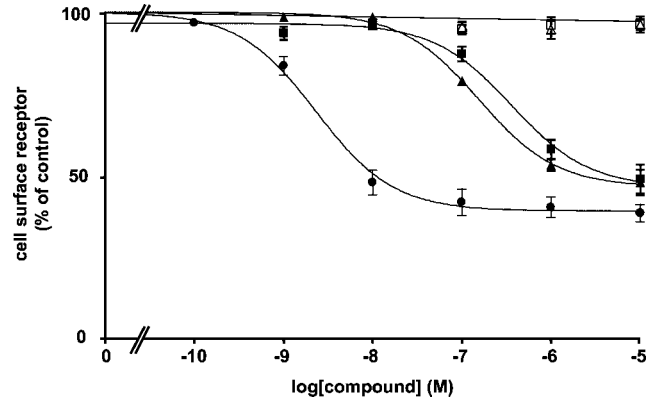

Figure 3. The SRIF analogues **32** and **8** behave like antagonists when tested in the ELISA-based internalization assay. HEK-sst$_2$ cells were preincubated with the mouse monoclonal HA epitope antibody (1:1000) at room temperature for 2 h and then processed for ELISA as described in Experimental Section. HEK-sst$_2$ cells were treated with 0.1 nmol/L, 1 nmol/L, 10 nmol/L, 100 nmol/L, 1 μmol/L, and 10 μmol/L [Tyr^3]octreotide (●) alone or with 1 nmol/L, 10 nmol/L, 100 nmol/L, 1 μmol/L, and 10 μmol/L [Tyr^3]octreotide in the presence of an increasing concentration (1 nmol/L, 10 nmol/L, 100 nmol/L, 1 μmol/L, and 10 μmol/L) of **32** (■) or the specific sst$_2$-antagonist **8** (▲). **32** and **8** are antagonists because they shift the dose dependent internalization curve of [Tyr^3]octreotide to a higher molar range. Tested alone at 100 nmol/L, 1 μmol/L, and 10 μmol/L, **32** (□) and **8** (△) do not stimulate sst$_2$ internalization in HEK-sst$_2$ cells.

instrument. The instrument employs a nitrogen laser (337 nm) at a repetition rate of 20 Hz. The applied accelerating voltage was 20 kV. Spectra were recorded in delayed extraction mode (300 ns delay). All spectra were recorded in the positive reflector mode. Spectra were sums of 100 laser shots. Matrix α-cyano-4-hydroxycinnamic acid was prepared as saturated solutions in 0.3% trifluoroacetic acid and 50% acetonitrile. The observed monoisotopic $(M + H)^+$ values of each peptide corresponded with the calculated $(M + H)^+$ values.

Reagents. All reagents were of the best grade available and were purchased from common suppliers. [Tyr^3]octreotide[41] was from Novartis Inc. (Basel, Switzerland). All other peptides, including **8**[27] were synthesized at the Salk Institute. The sst$_{2A}$-specific antibody R2-88 was generated as previously described and has been extensively characterized.[42] The secondary antibody Alexa Fluor 488 goat antirabbit IgG (H+L) was from Molecular Probes, Inc. (Eugene, OR), the monoclonal anti-T7 antibody from Novagen (Madison, WI), the goat antimouse IgG horseradish peroxidase conjugate from Bio-Rad Laboratories, Inc. (Hercules, OR). The Fluo-4NW calcium assay kit was from Molecular Probes, Inc. (Eugene, OR), substrate mix for horseradish peroxidase (ABTS) was from Bio-Rad Laboratories, Inc. (Hercules, OR), and lactalbumin hydrolysate was from HyClone (Logan, UT).

Cell Lines. CHO-K1, CCL39 cells stably expressing the cloned five human sst$_s$ and the HEK293 cell line expressing the T7-epitope tagged human sst$_{2A}$ (HEK-sst$_2$) were grown as described previously.[8,20] All culture reagents were from Gibco BRL, Life Technologies (Grand Island, NY).

Receptor Autoradiography. Cell membrane pellets were prepared as previously described[8] and stored at −80 °C. Receptor autoradiography was performed on 20 μm thick cryostat (Microm HM 500, Walldorf, Germany) sections of the membrane pellets, mounted on microscope slides, and then stored at −20 °C. For each of the tested compounds, complete displacement experiments with the universal SRIF radioligand [Leu^8,D-Trp^{22},^{125}I-Tyr^{25}]SRIF-28 (^{125}I-[LTT]SRIF-28) (2000 Ci/mmol; Anawa, Wangen, Switzerland) using 15 000 cpm/100 μL and increasing concentrations of the unlabeled peptide ranging from 0.1 to 1000 nM were performed. As control, unlabeled SRIF-28 was run in parallel using the same increasing concentrations. The sections were incubated with ^{125}I-[LTT]SRIF-28 for 2 h at room temperature in 170 mmol/L Tris-

HCl buffer (pH 8.2), containing 1% BSA, 40 mg/L bacitracin, and 10 mmol/L $MgCl_2$ to inhibit endogenous proteases. The incubated sections were washed twice for 5 min in cold 170 mmol/L Tris-HCl (pH 8.2) containing 0.25% BSA. After a brief dip in distilled water to remove excess salts, the sections were dried quickly and exposed for 1 week to Kodak BioMax MR film. IC_{50} values were calculated after quantification of the data using a computer-assisted image processing system as described previously.[43] Tissue standards (Autoradiographic [^{125}I] microscales, GE Healthcare; Little Chalfont, U.K.) that contain known amounts of isotope, cross-calibrated to tissue-equivalent ligand concentrations, were used for quantification.[44]

Immunofluorescence-Based sst_2 Internalization Assay. Immunofluorescence microscopy-based internalization assay for sst_2 was performed with HEK-sst_2 using the sst_2-specific antibody R2-88 as described earlier.[20] HEK-sst_2 cells were treated with vehicle alone, the sst_2 agonist [Tyr^3]octreotide at a concentration of 100 nM, [Tyr^3]octreotide at a concentration of 100 nM in the presence of an excess of the SRIF analogues to be tested (100 times the concentration of [Tyr^3]octreotide), or with the SRIF analogues to be tested alone at a concentration of 10 μM and then processed for immunofluorescence microscopy as described previously.[20]

Quantitative Assay for sst_2 Internalization (ELISA). Receptor internalization was determined using an ELISA to quantitate T7-epitope-tagged human sst_2 on the cell surface. HEK-sst_2 cells were seeded on poly-D-lysine (20 μg/mL) coated 24-well plates (250 000 cells per well) in growth medium and cultured for 1 day at 37 °C and 5% CO_2. On the day of the assay, cells were incubated with the monoclonal anti-T7 antibody at a dilution of 1:3000 for 2 h at room temperature in DMEM containing 5 g/L lactalbumin hydrolysate + 20 mM HEPES, pH 7.4 (DMEM-LH), to label cell surface receptors. After being washed with DMEM-LH to remove unbound antibody, cells were incubated for 30 min at 37 °C and 5% CO_2 either without or with the SRIF analogues to be tested, added at the concentrations indicated. Incubations were terminated by placing the plates in an ice bath. Cells were then washed twice with cold PBS and fixed for 10 min at room temperature with 3% paraformaldehyde in PBS (pH 7.4). Nonspecific binding sites were blocked by incubating the cells for 60 min at room temperature with PBS containing 1% bovine serum albumin (BSA, fraction V; SERVA, Heidelberg, Germany). Cells were then incubated for 60 min at room temperature with goat antimouse IgG horseradish peroxidase conjugate (1:1000) in PBS containing 1% BSA. After three additional washes with PBS, antibody binding was measured by adding 0.3 mL substrate mix for horseradish peroxidase (ABTS). The OD_{405} was measured after an approximately 30 min incubation at room temperature. The amount of sst_2 remaining at the cell surface after ligand treatment was calculated as the absorbance measured in treated cells expressed as a percentage of the absorbance in untreated cells. Nonspecific absorbance was determined in experiments in which HEK-sst_2 cells were incubated without the anti-T7 antibody. Each data point represents the mean ± SEM of three experiments performed in duplicate.

Calcium Release Assay. Intracellular calcium release was measured in HEK-sst_2 using the Fluo-4NW calcium assay kit as described previously.[45,46] In brief, HEK-sst_2 cells were seeded (25 000 cells per well) in poly-D-lysine (20 μg/mL) coated 96-well plates and cultured for 1 day at 37 °C and 5% CO_2 in culture medium. On the day of the experiment, the cells were washed with assay buffer (1× HBSS, 20 mM HEPES) containing 2.5 mM probenecid and then incubated with 100 μL/well Fluo-4NW dye in assay buffer containing 2.5 mM probenecid for 30 min at 37 °C and 5% CO_2 and an additional 30 min at room temperature. To measure the intracellular calcium mobilization after stimulation with the SRIF analogues to be tested, the dye-loaded cells were transferred to a SpectraMax M2^e (Molecular Devices, Sunnyvale, CA). Intracellular calcium mobilization was recorded in a kinetic experiment for 60 s at room temperature, monitoring fluorescence emission at 520 nm (with λ_{ex} = 485 nm) in the presence of the analogues at the concentrations indicated. Maximum fluorescence (F_{max}) was measured after the addition of 25 μM ionomycin. Baseline ($F_{baseline}$) measurements were taken for dye-loaded, untreated cells. Data are shown as percentage of maximum calcium response ($F_{max} - F_{baseline}$ = 100% of maximum calcium response) as reported previously.[45,46] All experiments were repeated at least three times in triplicate.

Acknowledgment. This work was supported in part by NIH Grant DK059953. We thank Dr. W. Fisher and W. Low for mass spectrometric analyses, R. Kaiser and C. Miller for technical assistance in the synthesis and characterization of some peptides. We are indebted to D. Doan for manuscript preparation. J.E.R. is the Dr. Frederik Paulsen Chair in Neurosciences Professor.

Supporting Information Available: CZE profiles of selected compounds. This material is available free of charge via the Internet at http://pubs.acs.org.

References

(1) Ginj, M.; Zhang, H.; Waser, B.; Cescato, R.; Wild, D.; Erchegyi, J.; Rivier, J.; Mäcke, H. R.; Reubi, J. C. Radiolabeled somatostatin receptor antagonists are preferable to agonists for in vivo peptide receptor targeting of tumors. *Proc. Natl. Acad. Sci. U.S.A.* **2006**, *103*, 16436–16441.

(2) Bass, R. T.; Buckwalter, B. L.; Patel, B. P.; Pausch, M. H.; Price, L. A.; Strnad, J.; Hadcock, J. R. Identification and characterization of novel somatostatin antagonists. *Mol. Pharmacol.* **1996**, *50*, 709–715.

(3) Bass, R. T.; Buckwalter, B. L.; Patel, B. P.; Pausch, M. H.; Price, L. A.; Strnad, J.; Hadcock, J. R. Identification and characterization of novel somatostatin antagonists. *Mol. Pharmacol.* **1997**, *51*, 170; Erratum.

(4) Hocart, S. J.; Jain, R.; Murphy, W. A.; Taylor, J. E.; Coy, D. H. Highly potent cyclic disulfide antagonists of somatostatin. *J. Med. Chem.* **1999**, *42*, 1863–1871.

(5) Bauer, W.; Briner, U.; Doepfner, W.; Haller, R.; Huguenin, R.; Marbach, P.; Petcher, T. J.; Pless, J. SMS 201-995: a very potent and selective octapeptide analog of somatostatin with prolonged action. *Life Sci.* **1982**, *31*, 1133–1140.

(6) Murphy, W. A.; Lance, V. A.; Moreau, S.; Moreau, J.-P.; Coy, D. H. Inhibition of rat prostate tumor growth by an octapeptide analog of somatostatin. *Life Sci.* **1987**, *40*, 2515–2522.

(7) Kwekkeboom, D.; Krenning, E. P.; de Jong, M. Peptide receptor imaging and therapy. *J. Nucl. Med.* **2000**, *41*, 1704–1713.

(8) Reubi, J. C.; Schaer, J. C.; Waser, B.; Wenger, S.; Heppeler, A.; Schmitt, J. S.; Mäcke, H. R. Affinity profiles for human somatostatin receptor sst1−sst5 of somatostatin radiotracers selected for scintigraphic and radiotherapeutic use. *Eur. J. Nucl. Med.* **2000**, *27*, 273–282.

(9) Kwekkeboom, D. J.; Bakker, W. H.; Kooij, P. P.; Konijnenberg, M. W.; Srinivasan, A.; Erion, J. L.; Schmidt, M. A.; Bugaj, J. L.; de Jong, M.; Krenning, E. P. [^{177}Lu-DOTAOTyr^3]octreotate: comparison with [^{111}In-DTPAo]octreotide in patients. *Eur. J. Nucl. Med.* **2001**, *28*, 1319–1325.

(10) Gulec, S. A.; Baum, R. Radio-guided surgery in neuroendocrine tumors. *J. Surg. Oncol.* **2007**, *96*, 309–315.

(11) Wild, D.; Schmitt, J. S.; Ginj, M.; Macke, H. R.; Bernard, B. F.; Krenning, E.; De Jong, M.; Wenger, S.; Reubi, J. C. DOTA-NOC, a high-affinity ligand of somatostatin receptor subtypes 2, 3 and 5 for labelling with various radiometals. *Eur. J. Nucl. Med. Mol. Imaging* **2003**, *30*, 1338–1347.

(12) Ginj, M.; Chen, J.; Walter, M. A.; Eltschinger, V.; Reubi, J. C.; Maecke, H. R. Preclinical evaluation of new and highly potent analogues of octreotide for predictive imaging and targeted radiotherapy. *Clin. Cancer Res.* **2005**, *11*, 1136–1145.

(13) Wehrmann, C.; Senftleben, S.; Zachert, C.; Muller, D.; Baum, R. P. Results of individual patient dosimetry in peptide receptor radionuclide therapy with ^{177}Lu DOTA-TATE and ^{177}Lu DOTA-NOC. *Cancer Biother. Radiopharm.* **2007**, *22*, 406–416.

(14) Gabriel, M.; Decristoforo, C.; Kendler, D.; Dobrozemsky, G.; Heute, D.; Uprimny, C.; Kovacs, P.; Von Guggenberg, E.; Bale, R.; Virgolini, I. J. ^{68}Ga-DOTA-Tyr^3-octreotide PET in neuroendocrine tumors: comparison with somatostatin receptor scintigraphy and CT. *J. Nucl. Med.* **2007**, *48*, 508–518.

(15) Van Essen, M.; Krenning, E. P.; De Jong, M.; Valkema, R.; Kwekkeboom, D. J. Peptide receptor radionuclide therapy with radiolabelled somatostatin analogues in patients with somatostatin receptor positive tumours. *Acta Oncol.* **2007**, *46*, 723–734.

(16) Kaltsas, G. A.; Papadogias, D.; Makras, P.; Grossman, A. B. Treatment of advanced neuroendocrine tumours with radiolabelled somatostatin analogues. *Endocr.-Relat. Cancer* **2005**, *12*, 683–699.

(17) Kwekkeboom, D. J.; Mueller-Brand, J.; Paganelli, G.; Anthony, L. B.; Pauwels, S.; Kvols, L. K.; O'Dorisio, T, M.; Valkema, R.; Bodei, L.; Chinol, M.; Maecke, H. R.; Krenning, E. P. Overview of results of peptide receptor radionuclide therapy with 3 radiolabeled somatostatin analogs. *J. Nucl. Med.* **2005**, *46*, 62S–66S.

(18) Kwekkeboom, D. J.; Teunissen, J. J.; Kam, B. L.; Valkema, R.; de Herder, W. W.; Krenning, E. P. Treatment of patients who have endocrine gastroenteropancreatic tumors with radiolabeled somatostatin analogues. *Hematol. Oncol. Clin. North Am.* **2007**, *21*, 561–573.

(19) Heppeler, A.; Froidevaux, S.; Eberle, A. N.; Maecke, H. R. Receptor targeting for tumor localisation and therapy with radiopeptides. *Curr. Med. Chem.* **2000**, *7*, 971–994.

(20) Cescato, R.; Schulz, S.; Waser, B.; Eltschinger, V.; Rivier, J. E.; Wester, H. J.; Culler, M.; Ginj, M.; Liu, Q.; Schonbrunn, A.; Reubi, J. C. Internalization of sst_2, sst_3, and sst_5 receptors: effects of somatostatin agonists and antagonists. *J. Nucl. Med.* **2006**, *47*, 502–511.

(21) Li, S.; Beheshti, M. The radionuclide molecular imaging and therapy of neuroendocrine tumors. *Curr. Cancer Drug Targets* **2005**, *5*, 139–148.

(22) Sundin, A.; Garske, U.; Orlefors, H. Nuclear imaging of neuroendocrine tumours. *Best Pract. Res. Clin. Endocrinol. Metab.* **2007**, *21*, 69–85.

(23) Forrer, F.; Valkema, R.; Kwekkeboom, D. J.; de Jong, M.; Krenning, E. P. Neuroendocrine tumors. Peptide receptor radionuclide therapy. *Best Pract. Res. Clin. Endocrinol. Metab.* **2007**, *21*, 111–129.

(24) Miller, C.; Rivier, J. Peptide chemistry: development of high-performance liquid chromatography and capillary zone electrophoresis. *Biopolym. Pept. Sci.* **1996**, *40*, 265–317.

(25) Miller, C.; Rivier, J. Analysis of synthetic peptides by capillary zone electrophoresis in organic/aqueous buffers. *J. Pept. Res.* **1998**, *51*, 444–451.

(26) Jiang, G.; Stalewski, J.; Galyean, R.; Dykert, J.; Schteingart, C.; Broqua, P.; Aebi, A.; Aubert, M. L.; Semple, G.; Robson, P.; Akinsanya, K.; Haigh, R.; Riviere, P.; Trojnar, J.; Junien, J. L.; Rivier, J. E. GnRH antagonists: a new generation of long acting analogues incorporating urea functions at positions 5 and 6. *J. Med. Chem.* **2001**, *44*, 453–467.

(27) Rajeswaran, W. G.; Hocart, S. J.; Murphy, W. A.; Taylor, J. E.; Coy, D. H. Highly potent and subtype selective ligands derived by *N*-methyl scan of a somatostatin antagonist. *J. Med. Chem.* **2001**, *44*, 1305–1311.

(28) Jiang, G.-C.; Simon, L.; Rivier, J. E. Orthogonally protected *N*-methyl-substituted α-aminoglycines. *Protein Pept. Lett.* **1996**, *3*, 219–224.

(29) Rivier, J. E.; Jiang, G.-C.; Koerber, S. C.; Porter, J.; Craig, A. G.; Hoeger, C. Betidamino acids: versatile and constrained scaffolds for drug discovery. *Proc. Natl. Acad. Sci. U.S.A.* **1996**, *93*, 2031–2036.

(30) Reubi, J. C.; Schaer, J.-C.; Wenger, S.; Hoeger, C.; Erchegyi, J.; Waser, B.; Rivier, J. SST3-selective potent peptidic somatostatin receptor antagonists. *Proc. Natl. Acad. Sci. U.S.A.* **2000**, *97*, 13973–13978.

(31) Erchegyi, J.; Wenger, S.; Waser, B.; Eltschinger, V.; Cescato, R.; Reubi, J. C.; Koerber, S. C.; Grace, R. C. R.; Riek, R.; Rivier, J. E. Use of Betidamino Acids in Drug Design. In *Understanding Biology Using Peptides. The 19th American Peptide Symposium*; American Peptide Society: San Diego, CA, 2005; pp 517−518.

(32) Chen, X.; Hou, Y.; Tohme, M.; Park, R.; Khankaldyyan, V.; Gonzales-Gomez, I.; Bading, J. R.; Laug, W. E.; Conti, P. S. Pegylated Arg-Gly-Asp peptide: ^{64}Cu labeling and PET imaging of brain tumor alphavbeta3-integrin expression. *J. Nucl. Med.* **2004**, *45*, 1776–1783.

(33) Antunes, P.; Ginj, M.; Zhang, H.; Waser, B.; Baum, R. P.; Reubi, J. C.; Maecke, H. Are radiogallium-labelled DOTA-conjugated somatostatin analogues superior to those labelled with other radiometals? *Eur. J. Nucl. Med. Mol. Imaging* **2007**, *34*, 982−993.

(34) Grace, C. R. R.; Erchegyi, J.; Koerber, S. C.; Reubi, J. C.; Rivier, J.; Riek, R. Novel sst_2-selective somatostatin agonists. Three-dimensional consensus structure by NMR. *J. Med. Chem.* **2006**, *49*, 4487–4496.

(35) Meyers, C. A.; Coy, D. H.; Huang, W. Y.; Schally, A. V.; Redding, T. W. Highly active position eight analogues of somatostatin and separation of peptide diastereomers by partition chromatography. *Biochemistry* **1978**, *17*, 2326–2330.

(36) Sypniewski, M.; Penke, B.; Simon, L.; Rivier, J. (*R*)-*tert*-Butoxycarbonylamino-fluorenylmethoxycarbonyl-glycine from (*S*)-benzyloxycarbonyl-serine or from papain resolution of the corresponding amide or methyl ester. *J. Org. Chem.* **2000**, *65*, 6595–6600.

(37) Stewart, J. M.; Young, J. D. *Solid Phase Peptide Synthesis*, 2nd ed.; Pierce Chemical Co.: Rockford, IL, 1984; p 176.

(38) Kaiser, E.; Colescott, R. L.; Bossinger, C. D.; Cook, P. I. Color test for detection of free terminal amino groups in the solid-phase synthesis of peptides. *Anal. Biochem.* **1970**, *34*, 595–598.

(39) Hoeger, C. A.; Galyean, R. F.; Boublik, J.; McClintock, R. A.; Rivier, J. E. Preparative reversed phase high performance liquid chromatography. II. Effects of buffer pH on the purification of synthetic peptides. *Biochromatography* **1987**, *2*, 134–142.

(40) Kaljuste, K.; Undén, A. New method for the synthesis of *N*-methyl amino acids containing peptides by reductive methylation of amino groups on the solid phase. *Int. J. Pept. Protein Res.* **1993**, *42*, 118–124.

(41) Reubi, J. C. Evidence for two somatostatin-14 receptor types in rat brain cortex. *Neurosci. Lett.* **1984**, *49*, 259–263.

(42) Gu, Y. Z.; Schonbrunn, A. Coupling specificity between somatostatin receptor sst2A and G proteins: isolation of the receptor−G protein complex with a receptor antibody. *Mol. Endocrinol.* **1997**, *11*, 527–537.

(43) Reubi, J. C.; Kvols, L. K.; Waser, B.; Nagorney, D.; Heitz, P. U.; Charboneau, J. W.; Reading, C. C.; Moertel, C. Detection of somatosatin receptors in surgical and percutaneous needle biopsy samples of carcinoids and islet cell carcinomas. *Cancer Res.* **1990**, *50*, 5969–5977.

(44) Reubi, J. C. In vitro identification of vasoactive intestinal peptide receptors in human tumors: implications for tumor imaging. *J. Nucl. Med.* **1995**, *36*, 1846–1853.

(45) Magrys, A.; Anekonda, T.; Ren, G.; Adamus, G. The role of anti-alpha-enolase autoantibodies in pathogenicity of autoimmune-mediated retinopathy. *J. Clin. Immunol.* **2007**, *27*, 181–192.

(46) Michel, N.; Ganter, K.; Venzke, S.; Bitzegeio, J.; Fackler, O. T.; Kepplet, O. T. The Nef protein of human immunodeficiency virus is a broad-spectrum modulator of chemokine receptor cell surface levels that acts independently of classical motifs for receptor endocytosis and Galphai signaling. *Mol. Biol. Cell* **2006**, *17*, 3578–3590.

JM701618Q